Assessment of temporal changes in aboveground forest tree biomass using aerial photographs and allometric equations

Avi Bar Massada, Yohay Carmel, Gilad Even Tzur, José M. Grünzweig, and Dan Yakir

Abstract: Studies of forest biomass dynamics typically use long-term forest inventory data, available in only a few places around the world. We present a method that uses photogrammetric measurements from aerial photographs as an alternative to time-series field measurements. We used photogrammetric methods to measure tree height and crown diameter, using four aerial photographs of Yatir Forest, a semi-arid forest in southern Israel, taken between 1978 and 2003. Height and crown-diameter measurements were transformed to biomass using an allometric equation generated from 28 harvested Aleppo pine (*Pinus halepensis* Mill.) trees. Mean tree biomass increased from 6.37 kg in 1978 to 97.01 kg in 2003. Mean plot biomass in 2003 was 2.48 kg/m^2 and aboveground primary productivity over the study period ranged between 0.14 and 0.21 kg/m^2 per year. There was systematic overestimation of tree height and systematic underestimation of crown diameter, which was corrected for at all time points between 1978 and 2003. The estimated biomass was significantly related to field-measured biomass, with an R^2 value of 0.78. This method may serve as an alternative to field sampling for studies of forest biomass dynamics, assuming that there is sufficient spatial and temporal coverage of the investigated area using high-quality aerial photography, and that the tree tops are distinguishable in the photographs.

Résumé : Les études de la dynamique de la biomasse forestière utilisent généralement des données d'inventaire forestier à long terme disponibles à quelques endroits seulement dans le monde. Nous présentons une méthode utilisant des mesures photogrammétriques tirées de photographies aériennes comme solution de rechange aux mesures de terrain répétées dans le temps. Nous avons utilisé des méthodes photogrammétriques pour mesurer la hauteur des arbres et le diamètre de leur cime à l'aide de quatre photographies aériennes prises entre 1978 et 2003 de la forêt de Yatir, une forêt semi-aride du sud d'Israël. Les mesures de hauteur et de diamètre de cime ont été converties en biomasse en utilisant une équation allométrique calculée à partir de l'abattage de 28 individus de pin d'Alep (*Pinus halepensis* Mill.). La biomasse moyenne des arbres a augmenté de 6,37 kg en 1978 à 97,01 kg en 2003. La biomasse moyenne des placettes en 2003 était de 2,48 kg/m^2 et la productivité primaire aérienne au cours de la période d'étude variait de 0,14 à 0,21 kg·m^{-2}·an^{-1}. Une surestimation systématique de la hauteur des arbres et une sous-estimation systématique du diamètre de la cime ont été corrigées pour toutes les mesures entre 1978 et 2003. La biomasse estimée était significativement reliée à la biomasse mesurée sur le terrain, ce qui a produit un R^2 de 0,78. Cette méthode peut servir de solution de rechange à un échantillonnage sur le terrain pour des études de la dynamique de la biomasse forestière en assumant que des photographies aériennes de haute qualité couvrent un horizon spatial et temporel suffisant pour la région étudiée et qu'il est possible de distinguer le faîte des arbres sur les photographies.

[Traduit par la Rédaction]

Introduction

Assessing aboveground biomass dynamics of forest trees is important for the estimation of long-term carbon storage, as well as for forest planning (Waring and Schlesinger 1985). Information on the dynamics of biomass accumulation in forests is critical, for example, for assessing its potential for long-term carbon sequestration. Detailed measurements of forest activity have been obtained over the last few years by eddy-correlation flux-tower measurements (Baldocchi et al. 2001; Hutley et al. 2005) that provide information on annual net ecosystem exchange (NEE) of CO_2 or net ecosystem productivity (NEP) when combined with estimates of ecosystem respiration losses (Janssens et al. 2003; Valentini et al. 2000). However, these measurements are limited to relatively short periods (years to decades). Typically, tree growth and biomass accumulation follow a

Received 15 December 2005. Accepted 2 June 2006. Published on the NRC Research Press Web site at http://cjfr.nrc.ca on 27 October 2006.

A. Bar Massada,[1] Y. Carmel, and G. Even Tzur. Faculty of Civil and Environmental Engineering, Technion – Israel Institute of Technology, Haifa 32000, Israel.
J.M. Grünzweig[2] and D. Yakir. Department of Environmental Sciences and Energy Research, Weizmann Institute of Science, Rehovot 76100, Israel.

[1]Corresponding author (e-mail: agavi@tx.technion.ac.il).
[2]Present address: Institute of Plant Science and Genetics in Agriculture, Faculty of Agricultural, Food and Enviromental Quality Sciences, The Hebrew University of Jerusalem, Rehovot 76100, Israel.

 doi:10.1139/X06-152

saturation curve (Barnes et al. 1998). An establishment period is followed by a period of nearly linear biomass accumulation over time, and finally by a decreasing rate of biomass accumulation as the forest approaches maturity and the ratio between photosynthesis and respiration decreases. Coupling detailed flux measurements with long-term biomass dynamics can be particularly useful in indicating the perspective of the short-term measurements in the life cycle of the forest ecosystem. For example, the meaning and local or regional predictions of net ecosystem productivity will be different if the forest is at its linear growth rate stage, near maturation and steady state, or during a transition to forest decline.

Aboveground forest biomass dynamics are commonly estimated using field measurements in permanent study plots. The determination of biomass typically involves measurements of tree size parameters such as trunk diameter at breast height (DBH) and tree height. These parameters are converted to biomass using empirical allometric equations (Parresol 1999; Waring and Schlesinger 1985; West et al. 1997).

Long-term biomass data calculated from field measurements exist for only a few places around the world (Birdsey and Lewis 1997; Birdsey and Schreuder 1992; Fang et al. 2001; Fang and Wang 2001). For places where such data are unavailable, it is desirable to find an alternative approach to assess the long-term dynamics of tree biomass. In the past 25 years, remote-sensing techniques have emerged as a promising alternative. Examples include radar (synthetic aperature radar, SAR) (Beaudoin et al. 1994; Del Frate and Solimini 2004; Ranson et al. 1997; Tsolomon et al. 2002), lidar (Nelson et al. 1988; Nelson et al. 1997), and the fusion of a number of remote-sensing sources (Baccini et al. 2004; Svoray and Shoshany 2003; Treuhaft et al. 2003). However, promising as these methods may be, they still suffer from a major limitation: the time frame is too short to assess biomass dynamics.

An alternative source of biomass data are aerial photographs, which in many places have extensive spatial and temporal coverage. Forest-inventory procedures using aerial photography have been common since the mid-20th century. They include stand-level measurements, such as volume (Aldred and Lowe 1978; Bonnor 1977), cover and distribution (Hudak and Wessman 1998; Kadmon and Harari-Kremer 1999), canopy structure (Nakashizuka et al. 1995), stand biomass (Fensham et al. 2002; Okuda et al. 2004), and individual-tree-level measurements, such as tree position, height, crown diameter/area, tree species, and allometric estimation of trunk dimensions (Gong et al. 2002; Korpela 2004; Larsen and Rudemo 1998; St-Onge et al. 2004). To the best of our knowledge, tree-level measurements have not so far included the temporal dynamics of tree biomass data. This is partly because the main biomass predictor, DBH, cannot be measured from aerial photographs because of canopy obstruction. However, other 3D tree parameters can be measured from aerial photographs. These are crown-related parameters, such as tree-top position and crown radius/diameter (Gong et al. 2002; Korpela 2004; Kovats 1997; St-Onge et al. 2004). Korpela (2004) combined photogrammetrically measured tree height, tree crown diameter, and tree species with allometric species-specific models to estimate DBH, and used a taper curve of the stem for volume calculations. Okuda et al. (2004) studied height to DBH relations and then estimated the total aboveground tree biomass of a tropical forest by relating the mean height of the canopy-forming trees (measured by photogrammetric methods) to the field-measured biomass of those trees. Okuda et al. (2004) avoided estimating single-tree biomass, focusing instead on stand-level characteristics. Both Korpela (2004) and Okuda et al. (2004) found significant relations between tree height and DBH. Given that DBH is strongly related to biomass, this is essentially equivalent to estimating aboveground tree biomass, thus highlighting the potential for directly relating tree size (height and crown diameter) to tree biomass via an allometric equation.

The main objective of this study is to develop a method for estimating the temporal dynamics of aboveground forest biomass. The method is based on multitemporal photogrammetric measurements of tree height and crown diameter and a corresponding allometric equation that converts these values to tree biomass. A secondary objective is to apply this method to assess aboveground tree biomass and stand biomass dynamics in the footprint of an eddy-correlation flux tower in Yatir Forest, southern Israel, for a period of 25 years.

The major advantage of this method is the potential for reconstructing time series of biomass estimates. The dynamics of Yatir Forest biomass greatly extend the information obtained by making continuous carbon flux measurements at the Yatir site over the past 4 years (Grünzweig et al. 2003). Combined, the current annual carbon uptake of the forest can be put in the context of the forest life cycle and improve the accuracy of predictions of future wood production and carbon sequestration.

Materials and methods

Study area

Yatir Forest is the largest planted forest in Israel, covering an area of about 2800 ha, with mostly (over 90%) Aleppo pine, *Pinus halepensis* Mill. The forest topography is hilly, with an average elevation of ~650 m above sea level. The elevation rises gradually from ~550 m in the western part of the forest to ~800 m at its eastern edge. The climate is semi-arid, with 280 mm annual mean precipitation during the last 30 years. *Pinus halepensis* trees in Yatir Forest reach a maximal height of ~20 m. At present, the canopy is barely closed (i.e., there are not many trees with interlaced crowns), thus the ground is visible from above in many places in the forest. There is little understorey vegetation. The forest was subjected to regular thinning of approximately 30% of the trees every 7 years. There is no natural regeneration of trees, probably because of the climatic conditions, which are much drier than elsewhere within the species' distribution range. A more detailed description of the forest can be found in Grünzweig et al. (2003).

The study area is located in the oldest part of the forest, planted in the mid-1960s. This area represents the main footprint of the 18 m high flux tower used for continuous measurements of fluxes of CO_2, water vapor, and energy between the forest and the atmosphere over the past 4 years. Ten 30 m × 30 m plots (Fig. 1) were selected within the

Fig. 1. The study area and study plots (rectangles 1–10). The 10 m elevation contours are outlined in white. The stand in the photograph consists mostly of 40-year-old *Pinus halepensis* Mill. The 10 study plots cover 30 m × 30 m. The photograph (scale 1 : 13 000) was taken on 4 July 2003 at 11:46 a.m. from a height of ~2100 m.

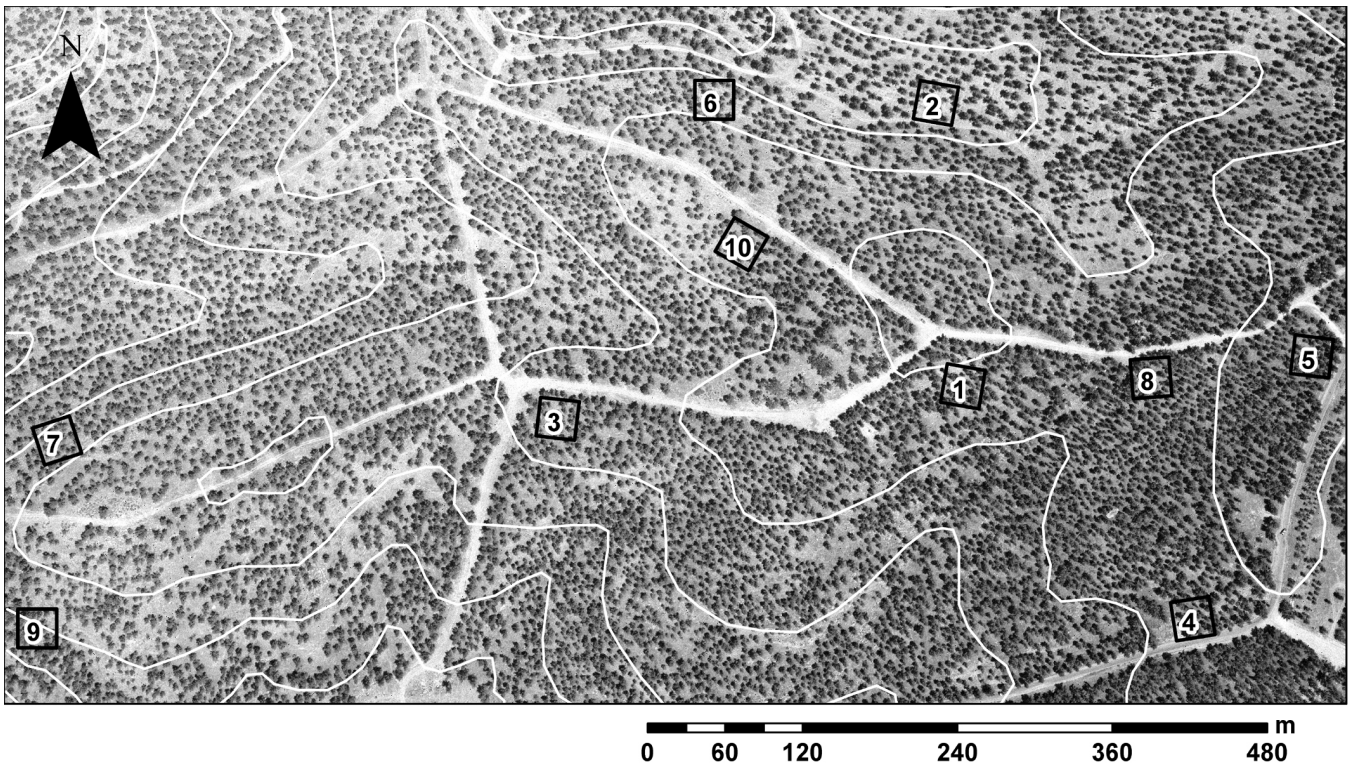

study site to represent the variability in tree density and ground slope across the study area (Table 1), since all trees are of the same age. All trees within each plot were measured during the study; the number of trees visible in older photographs was greater because some were later removed by thinning. Large plots were used to compensate for the relatively small number of plots. Results from this study will be used later as a component in the validation of the flux-tower measurements. However, the validation process is beyond the scope of this paper.

Table 1. Details of the 10 sample plots in the study area.

Plot	Mean elevation (m a.s.l.)	Mean slope (°)	No. of trees	Density (trees/ha)
1	657.73	0.95	28	311
2	636.39	1.01	17	189
3	643.81	3.84	29	322
4	654.92	6.40	19	211
5	665.01	3.58	30	333
6	645.25	14.07	19	211
7	623.90	16.63	25	278
8	655.84	3.81	23	256
9	618.62	15.18	23	256
10	655.64	2.30	21	233

Aerial photographs

Four sets of scanned panchromatic aerial photographs of an area in the center of Yatir Forest (in 1978, 1987, 1992, and 1996) were purchased from the Survey of Israel, and a new pair of photographs with the same characteristics was obtained in 2003 following an aerial survey of the study area. Each set consists of a pair of 1 : 13 000 scale photographs with 60% overlap (Table 2). Twelve ground control points (large rocks evident in all images), distributed uniformly throughout the study area, were measured with an Ashtech Z Surveyor GPS using the differential method (Seeber 1993). The image pairs from all years were solved (interior and exterior orientation) in ERDAS IMAGINE OrthoBASE® version 8.6 software using the photographs, the corresponding camera calibration parameters (supplied by the manufacturer), the ground control points, and 30 tie points. The solution method was standard bundle block adjustment, which was applied separately to each year of photograph acquisition (a total of five solutions). After solving the exterior orientation of each stereo-pair, orthophotographs were generated separately for each year, using corresponding digital elevation models (DEM).

The total unit-weight root mean square errors (RMSE) of the solutions were intermediate (Table 2), with an exceptionally high value (2.15 m) in 1992 (probably because of the low quality of the 1992 photographs, which hindered identification of the locations of the ground control points). Thus, the 1992 photographs were omitted from the study (see the Discussion for details).

Photogrammetric height and crown-diameter measurements

Tree height was measured photogrammetrically in ERDAS IMAGINE Stereo Analyst® version 8.6 software. The 3D positions of tree tops were digitized manually using

Table 2. Image characteristics and parameters of the solutions of the image pairs by bundle block adjustment.

			RMSE						
Year	Camera type	Photographic scale	Scanning resolution (dpi)	Ground X (m)*	Ground Y (m)*	Ground Z (m)*	Image X (pixels)†	Image Y (pixels)†	Total (m)‡
1978	Wild RC 8	1 : 13 000	2117	3.68	0.94	0.47	0.03	0.57	0.64
1987	Wild RC 20	1 : 13 000	2016	0.04	0.02	0.06	0.76	0.61	0.59
1992	Wild RC 20	1 : 13 000	2117	1.04	0.57	1.95	0.08	0.91	2.15
1996	Wild RC 30	1 : 13 000	2016	0.01	0.00	0.01	0.08	0.10	0.37
2003	Zeiss RMK TOP 15	1 : 12 500	1800	0.09	0.18	0.16	0.15	0.28	0.38

*RMSE of the location errors of the ground control points in object coordinates.
†RMSE of the location errors of the ground control points in image coordinates.
‡Unit-weight RMSE of the ground control point locations in object coordinates.

monoscopic viewing of images that had been normalized for stereo (i.e., images in which corresponding entities appear in the same image rows, i.e., epipolar images). Two image-point measurements in the epipolar images yield 3D coordinates (position) for the tree tops by forward ray intersection. Since the Z coordinate of the tree top was its elevation above sea level, it was necessary to measure the ground elevation below the tree. However, the canopy obstructed most of the ground near the trees, so ground elevation below the trees had to be estimated rather than measured directly. This was done by generating a DEM for all plots in all image pairs. Ground points were measured in gaps between canopies, where shadows of crowns cast on the ground were easily identifiable. The number of ground points per plot varied between 8 (in very dense plots) and 37 (in open plots) depending on the amount of ground surface not obscured by trees. DEMs were then generated by applying a linear rubber sheeting interpolation to the ground points (ERDAS Inc. 1999). Ground elevation below each tree was then estimated from the DEM, given the photogrammetric XY coordinates of the tree apex. DEMs were generated for each year independently. This additional work was done to minimize the effect of error in the photogrammetric solutions (see the Discussion).

Tree crown diameter was measured in ArcGIS® version 8.2 software by digitizing it as a line in the orthophotographs. In the case of off-nadir trees, digitization followed the maximal visible diameter of the crown that was perpendicular to an imaginary line connecting the tree top and the ground. In measuring both height and crown diameter the growth of specific trees was not followed in images from different years, as the main focus in this study was the average characteristics of the stand (mean tree biomass and plot biomass), not the growth of individual trees.

Error assessment

Error in tree height and crown-diameter measurements was estimated empirically in an independent validation plot in the study area in 2003, 1 month after photo-acquisition. The plot consisted of 60 trees that were measured for height and crown diameter both in the images and in the field. Each tree in the image was carefully identified in the field (image hard copies were taken to the field and trees were identified one by one). Actual tree height was measured with a clinometer and a tape. Crown diameter was measured with a compass and a tape according to the digitizing angle of each tree on the 2003 orthophotograph. Measurement errors were calculated as the difference between photogrammetric measurement and field measurement, assuming that the errors in the field measurements were negligible. In addition to size measurements, the biomass of the 60 trees was calculated using the selected allometric equation, and the relation between field-measured biomass and photogrammetrically estimated biomass was assessed.

The empirical error assessment could only be applied to image measurements for which there were corresponding field measurements (i.e., the 2003 set). Thus, it was desirable to assess whether the measurement errors were the same for older images, where no field data were available. A prerequisite for using current error measurements for correcting measurements in older images is that measurement error is independent of tree size (since trees were younger and smaller in older photographs). In that case, mean measurement errors might be used as calibrating factors for all height and crown-diameter measurements done in the study. Regression analysis was used to test the relation between measurement error and tree size (i.e., the relation between height measurement error and actual height, between crown diameter measurement error and actual crown diameter), and between field-measured biomass and photogrammetrically measured biomass.

Generation of allometric equations

The allometric equations were based on a sample of 28 *P. halepensis* trees that were harvested, dried, and weighed in July 2004 to determine tree biomass. The trees were selected from various parts of the forest representing a wide array of age classes. Prior to harvest, an inventory of height and DBH for 257 trees was performed in the forest. A polynomial regression equation ($R^2 = 0.58$) was fitted to the data to determine the average height/DBH relation in the forest. Only trees that had a good fit to the equation were selected for harvesting, to prevent any effect of outliers on the small sample size.

Biomass, height, and crown diameter of each tree were used to generate a log-transformed allometric equation (since linear allometric equations suffer from heteroscedasticity). The equation was corrected for an inherent bias in log-transformed allometric equations using Sprugel's correction factor (Sprugel 1983).

Biomass calculations

Calibrated tree height and calibrated tree crown diameter data from all four time points were incorporated into the se-

lected allometric equation to yield tree biomass data. Mean tree biomass (per plot for all time points) and mean plot biomass (per year) were regressed against tree density and mean ground slope (since increased runoff on steeper slopes might decrease water availability for trees in arid environments, resulting in lower growth rates).

Analysis of the temporal dynamics of plot biomass in Yatir Forest must also consider the biomass removed between time points. Plot biomass dynamics are strongly influenced by the thinning practices in the forest. An average rate of biomass production over the entire 25 year period was estimated as follows

$$[1] \qquad B_p = \frac{\overline{B}_{2003} - \overline{B}_{1978} + B_r}{25}$$

where B_p is the mean annual production rate of tree biomass per unit area (kg/m^2 per year), $\overline{B}_{2003}$ and $\overline{B}_{1978}$ are the mean plot biomass values (kg/m^2) in 2003 and 1978, respectively, and B_r is the total amount of biomass removed per unit area throughout the corresponding 25 years (kg/m^2). The amount of biomass removed between samplings was estimated using three alternative scenarios regarding the actual timing of thinning: (1) immediately after the earlier sampling, (2) between two samplings, and (3) before the following sampling. In the first and third scenarios the amount was calculated as mean tree biomass at the nearest sampling period multiplied by the mean number of trees removed between two samplings (where the number of trees removed is the difference in tree counts between successive samplings). In the second scenario the amount was calculated as the average mean biomass of the samples multiplied by the mean number of trees removed. Three estimates of the total amount of biomass removed were generated by summing the amounts from all periods for each thinning scenario. This procedure yielded three estimates of the average biomass-production rate and could be used for a first approximation of the possible error involved.

Results

Error assessment

The empirical error assessment showed that height error and crown-diameter error were quite low (about 10% of the real tree dimensions). Mean height error for 60 trees was 0.76 m and mean crown-diameter error was –0.47 m (Table 3). Tree height was usually overestimated, as 44 of 60 error values were positive (tree height measured from the image was greater than field-measured tree height), while tree crown diameter was usually underestimated, as 53 error values were negative (Fig. 2). The regression between height error and tree height was not significant, nor was the regression between crown-diameter error and tree crown diameter (Fig. 3). Since there was no relation between tree size and measurement error, the mean errors were used as calibrating factors for all tree measurements in this study. To correct the overestimation, 0.76 m was subtracted from each height measurement in the study (in all years). To correct the underestimation, 0.47 m was added to each crown-diameter measurement in the study (all years). A single correction value was applied to different-sized trees throughout the study, as it was found that height error was independent of tree size.

Table 3. Error indices of height, crown diameter, and tree biomass for the 60 trees in the independent validation plot.

	Mean error	Mean absolute error	RMSE
Tree height (m)	0.76	1.33	1.624
Crown diameter (m)	–0.47	0.56	0.671
Biomass (kg)	–1.82	25.34	34.31

Fig. 2. Distribution of height errors (shaded bars) and crown-diameter errors (solid bars) from the error-assessment procedure in which 60 trees were measured both in the field and by computer (using photogrammetric methods). Negative error values correspond to cases where the field measurements were higher than the computer measurements, therefore the method underestimated the measured values, and vice versa for positive errors.

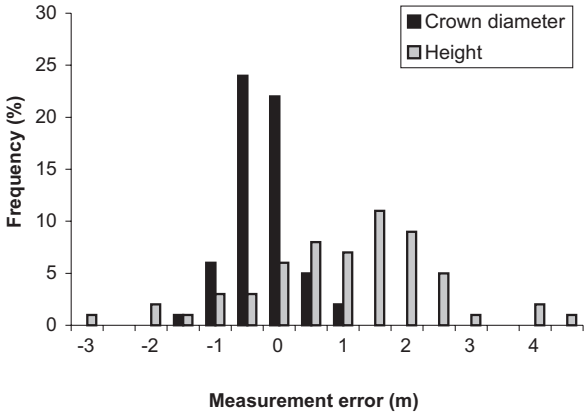

The mean biomass error was small, –1.82 kg, but the mean absolute error and RMSE were higher (Table 3). The regression between model biomass and field-measured biomass in the 60 trees of the validation plot was highly significant ($p < 0.001$), with $R^2 = 0.78$ (Fig. 4).

Generation of allometric equations

The allometric equation using tree height and crown diameter as biomass predictors is shown in eq. 2.

$$[2] \qquad \ln B = \underset{(0.21)}{-1.35} + \underset{(0.24)}{1.48} \ln \mathrm{CD} + \underset{(0.23)}{1.67} \ln H$$

$$(R^2 = 0.98,\ p < 0.001,\ \mathrm{CF} = 1.0197)$$

where B is tree biomass (kg dry mass), CD is crown diameter (m), and H is tree height (m). The numbers in parentheses below the coefficients are their standard errors. CF is Sprugel's correction factor (Sprugel 1983).

Tree characteristics

Mean tree height increased over the study period, and growth rates (change of height over time) declined (Fig. 5). Mean tree height in 2003 was 9.72 m. There was large variability in mean tree height among the study plots, ranging from a maximum difference of 2.5 m (134%) in 1978 to 3.7 m (49%) in 2003. In most years plot 10 had the lowest mean tree height and plot 4 had the highest trees. Height

Fig. 3. Relations between the photogrammetric measurement error of crown diameter and real crown diameter (top) and between the photogrammetric measurement error of tree height and real height (bottom) for the 60 trees in the independent validation plot.

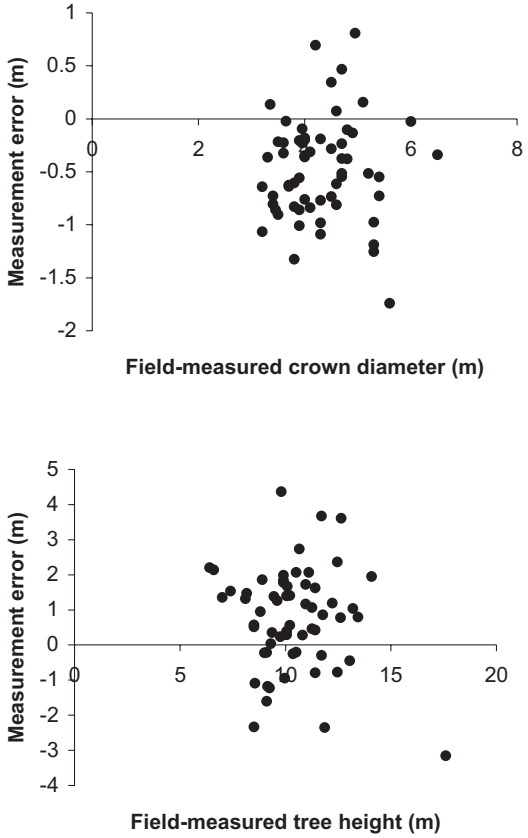

Fig. 4. Relation between model-estimated biomass (based on photogrammetric measurements of tree height and crown diameter) and field-estimated biomass for the 60 trees in the independent validation plot.

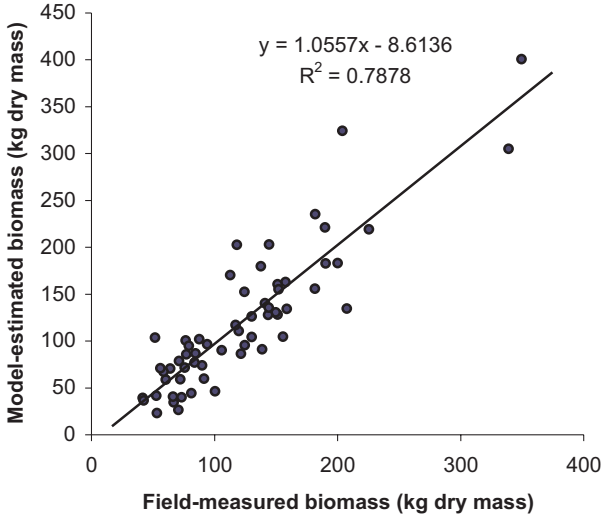

Fig. 5. Temporal dynamics of mean tree height and its standard deviation measured from the aerial photographs. Mean tree height was calculated for all trees in all plots for each measurement year.

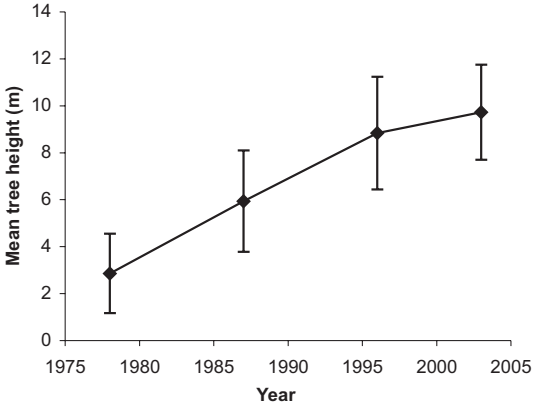

measurements in plot 3 were difficult to make in 1987 and 1996, probably because of the high density of the trees, which created a closed canopy, hindering the identification of matching tree tops in the image pair. Therefore, these results were omitted from the statistical analysis. The regression between mean tree height and ground slope in the study plots was not significant. Mean tree crown diameter increased gradually from 2.09 m in 1978 to 3.66 m in 2003. Differences in mean crown diameter between plots were smaller than differences in height, ranging from 0.63 m (33%) in 1978 to 0.82 m (25%) in 2003.

The number of trees in the study plots decreased during the study period, predominantly as a result of thinning practices. The mean number of trees per plot decreased from 74 in 1978 to 23 in 2003 (Fig. 6). The variability in the number of trees per plot decreased through the years (Fig. 6), most likely as a result of the thinning strategy.

Tree and plot biomass

Tree biomass was calculated for a total of 1857 observations at four time points, using calibrated height and crown-diameter data. Mean plot biomass in the study area was 2.48 kg/m^2 in 2003, with mean tree biomass of 97.01 kg. Mean tree biomass varied greatly among plots over the years. Mean annual growth rate of tree biomass also increased from 1.63 kg/year for 1978–1987 through 3.8 kg/year for 1987–1996 to 5.95 kg/year for 1996–2003 (Fig. 6). Considering biomass removal using scenarios 1, 2, and 3 indicated mean biomass production rates of 0.14, 0.17, and 0.21 kg/m^2 per year, respectively (see Materials and methods). About 44%, 55%, and 63% of the biomass produced in 25 years was removed by thinning treatments, assuming scenarios 1, 2, and 3, respectively. Mean plot biomass and the partitioning between standing and removed tree biomass are plotted in Fig. 7.

The relation between tree biomass and mean ground slope, plot density, or a combination of the two was variable. Stand density was almost always a significant predictor of biomass. However, the regression statistic R^2 was always very low (<0.1). In contrast, ground slope was never a significant predictor of biomass.

Fig. 6. Temporal dynamics of mean tree biomass (all plots combined) and mean number of trees per plot. Values on the *y*-axis correspond to both parameters. The error bars denote standard deviation.

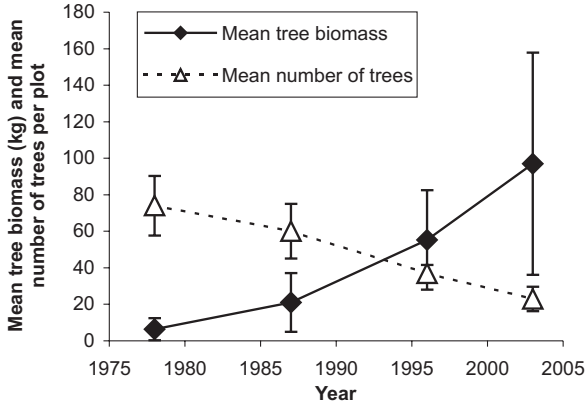

Fig. 7. Mean plot biomass at different years. Standing biomass at the time of measurement is based on mean plot biomass for all plots in the study area. Removal of biomass occurred during periodic thinning (scenario 2). The error bars denote the assumptions of the two extreme thinning scenarios (thinning at the beginning (scenario 1) or the end (scenario 3) of the measurement time step).

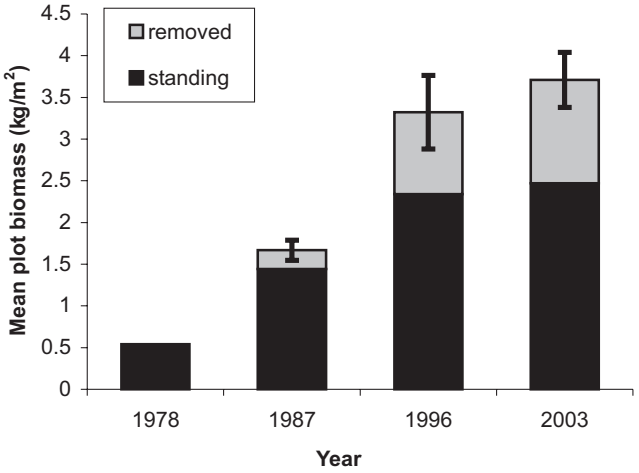

Discussion

The method

The approach developed and applied in this work allows aboveground biomass to be calculated for individual trees in a forest to determine the change in mean tree biomass and stand biomass, and ultimately to estimate biomass-production rates for an entire forest. For this method to work successfully, two requirements had to be met. (1) Parameters corresponding to tree biomass needed to be estimated accurately from aerial photographs. In this study, tree height and crown diameter were estimated from aerial photographs and reasonable accuracy was achieved (compared with other works, e.g., Gong et al. 2002; Kovats 1997). (2) Close correspondence between measurable tree parameters and tree biomass is required. In this study the log-transformed allometric equation that incorporates both tree height and crown diameter met this requirement, the adjusted R^2 value being 0.98. Such strong relations were achieved previously only when DBH was one of the predictors (Deans et al. 1996; Ritson and Sochacki 2003; Son et al. 2001). This is important, as DBH cannot be obtained directly from aerial photographs. The strong relations between tree height, crown diameter, and tree biomass highlight the potential usefulness of aerial photography for compiling a forest-biomass inventory.

The RMSE of the control points in the triangulation process was intermediate, except in the 1992 image pair, where it was high. The large error in 1992 was probably due to the low quality of the corresponding images, which hindered the identification of the image locations of the ground control points and further reduced the accuracy of the photogrammetric solution. As a result the 1992 image pair was removed from the study. This is a potential drawback of the method, since it is probable that not all available photographs will have the high quality necessary for the photogrammetric solution.

The decision to generate separate DEMs for each year was taken as a precaution, to minimize the effect of non-negligible errors in the photogrammetric solutions.

The systematic underestimation of tree crown diameter and systematic overestimation of tree height apparent in the results of the empirical error assessment in this study cannot be adequately explained. The absence of any significant relation between measurement errors and tree size, also reported by St-Onge et at. (2004), leads to the conclusion that the governing determinant of measurement accuracy was the "clarity", or image quality, rather than tree size. The quality of the result depended on the operator's ability to accurately locate the tree apex in both images. This, in turn, depended on two factors: whether the tree had any clear apex and whether the image quality was good enough that this apex could be clearly distinguished from its surroundings. *Pinus halepensis* trees are especially difficult in this respect, since their crown morphology tends to be complex (Fig. 8). It is easier to locate the tree apex in side (non-nadir) views than in the nadir view (Gong et al. 2002), since apex identification in the nadir view is based on the location of the brighter pixels (Fig. 8). The higher parts of trees tend to appear brighter than their surroundings in aerial photographs, since these parts receive more light. When the real apex is sharp and clear, it appears as a bright point in the tree. If there is no clear apex, an entire area in the tree crown appears brighter in the nadir view. In such cases, the apex was selected as close as possible to the center of the tree, assuming that the highest point in the tree is in its center.

Another potential source of error in height estimates is the quality of the DEM, since tree height is calculated as the difference between absolute height and ground height obtained from the DEM. In dense stands, where the ground surface is obstructed by the canopy, the number of potential ground points available for DEM generation is low. This might bias the estimates of ground height in the DEM, which may reduce the accuracy of tree-height estimates. This problem can be solved by generating the ground DEM using lidar measurements (Okuda et al. 2004; St-Onge et at. 2004), which are possibly more accurate than canopy-gap-dependent photogrammetric measurements.

Fig. 8. Left, nadir, and right views of trees in Yatir Forest from three overlapping aerial photographs, illustrating the difficulty of measuring height and crown diameter. For height measurements, identifying the tree apex in the nadir view is much more difficult than identifying it in side views. In contrast, crown diameter is easily identified in the nadir view and difficult to identify in side views.

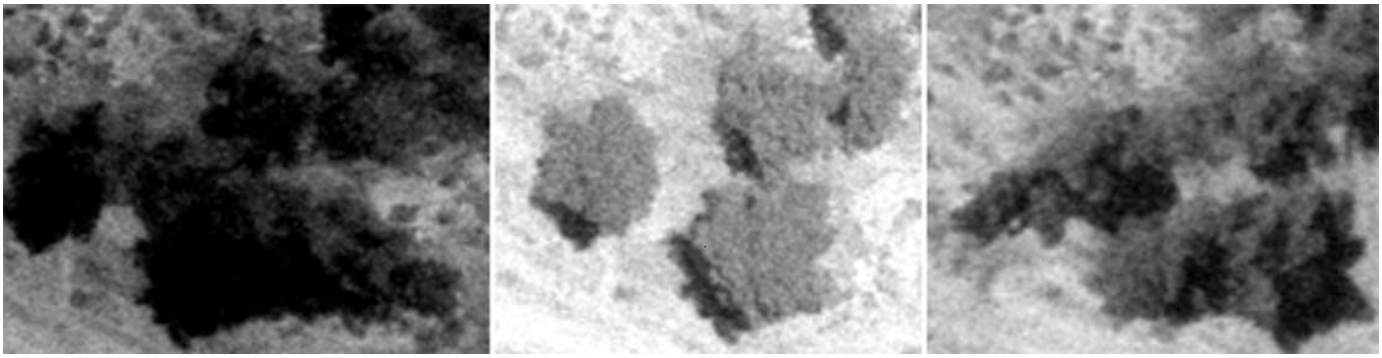

The major source of error in crown-diameter measurements is the off-nadir viewing of the trees. The best way to measure diameter is in the nadir view, where the tree appears nearly circular. In non-nadir views only one possible crown diameter is visible: the one perpendicular to the imaginary line connecting the crown center to the ground. The farther the view is from the nadir, the greater the chance that some tree crowns will be hidden behind larger trees.

Taking into account these inherent problems, Gong et al. (2002) based their tree measurements on three photographs rather than two as in this study. Tree heights were measured in left and right views and the crown radius was measured in the nadir view. They report a mean absolute error in tree height of 1.8 m. In this work the mean absolute error (1.3 m) was lower, even though only two photographs were used in the process.

The difficulty of measuring in plot 3 revealed another potential drawback of the method: in stands where there is complete canopy closure (no gaps), and that consist of trees with nearly flat crown tops, it is nearly impossible to identify individual tree tops. This hindrance prevented photogrammetric measurements in three cases in this study. However, in the majority of cases, the unclosed canopy formation counteracted the problematic crown morphology of *P. halepensis* trees. Thus, it is concluded that the applicability of the measurements in this method depends on the interaction between two factors: the morphology of the canopy top and the degree of canopy closure of the stand.

Finally, using this method for multispecies stands may be prohibitively difficult. It would demand the use of various allometric equations rather than a single equation as in Yatir Forest. In such cases it is also desirable to develop a classification technique that will differentiate between trees of different species.

A strong correlation was found between tree height, crown diameter, and tree biomass. This is partly due to the method of selecting the trees used in generating the allometric equation. These trees were selected along a regression curve between height and DBH calculated from a large data set of trees in the forest. DBH is known to be a good predictor of biomass; hence, a strong relation between height and biomass is not surprising. However, the allometric equation included another significant predictor, crown diameter, that was not accounted for in the selection process. Thus, the high significance of the allometric equation is probably not solely a result of the selection process.

The Yatir Forest case study

Yatir Forest is a unique semi-arid forest that shows unexpectedly high NEE values (Grünzweig et al. 2003) over the past 4 years. The additional long-term perspective obtained in the present study shows that these measurements represent the near-linear growth stage of the forest, and that even after 40 years of growth under dry conditions, there is no indication of equilibrium or steady state.

Yatir Forest, like most managed forests, is influenced by management activities in addition to natural processes. In this case, the main management activity is thinning, aimed at maintaining the forest at a density that could be sustained by the low precipitation. Therefore, the description of plot biomass dynamics using solely the observed measurements does not portray the actual fluctuations in the accumulated plot biomass. Here it has been shown that it is possible to account for the effect of thinning by estimating the amount of biomass removed in each thinning event by comparing consecutive aerial photographs of the same plot and applying the methodology for estimating biomass presented here to the missing trees in each time step. The results reveal that the biomass removed by thinning was indeed a significant component of total accumulated plot biomass (between 46% and 60% depending on the thinning scenario). After accounting for the amount of biomass removed, the rate of biomass accumulation in Yatir Forest was 1.4–2.1 t/ha per year (within the range reported for other arid-land forests; see Barnes 1998). This indicates that the forest is not in a steady state, and that accumulation rates have increased in recent years (Figs. 7 and 8). This provides support for the significant carbon sink calculated from the extensive flux measurements made at the site over the past several years (total ecosystem uptake >2 tons/ha, including belowground accumulation; see Grünzweig et al. 2003).

Conclusions

The methodological approach presented here offers a simple and fast way to estimate the temporal dynamics of forest biomass when historical forest inventories are unavailable. Several promising methods to automatically estimate biomass have been developed in recent years. However, they all

share the same constraint: they rely on data sources that do not yet cover a long enough time span, so they cannot be used to estimate long-term changes in biomass. In contrast, the approach developed in this study makes use of aerial photographs as the source for tree measurements. Depending on the temporal and spatial availability of historical aerial photography (and the quality and scale of available photographs, combined with the characteristics of the stand of interest), this method might be an applicable tool for assessing the temporal dynamics of forest biomass, and prove useful for foresters as well as ecologists.

References

Baccini, A., Friedl, M.A., Woodcock, C.E., and Warbington, R. 2004. Forest biomass estimation over regional scales using multisource data. Geophys. Res. Lett. **31**: L10501. doi: 10.1029/2004GL019782.

Baldocchi, D., Falge, E., and Gu, L. 2001. FLUXNET: a new tool to study the temporal and spatial variablility of ecosystem-scale carbon dioxide, water vapor, and energy flux densities. Bull. Am. Meteorol. Soc. **82**: 2415–3434.

Barnes, B.V., Zak, D.R., Denton, S.R., and Spurr, S.H. 1998. Forest ecology. 4th ed. John Wiley & Sons, New York.

Beaudoin, A., Letoan, T., Goze, S., Nezry, E., Lopes, A., Mougin, E., Hsu, C.C., Han, H.C., Kong, J.A., and Shin, R.T. 1994. Retrieval of forest biomass from SAR data. Int. J. Remote Sens. **15**: 2777–2796.

Deans, J.D., Moran, J., and Grace, J. 1996. Biomass relationships for tree species in regenerating semi-deciduous tropical moist forest in Cameroon. For. Ecol. Manage. **88**: 215–225.

Del Frate, F., and Solimini, D. 2004. On neural network algorithms for retrieving forest biomass from SAR data. IEEE Trans. Geosci. Remote Sens. **42**: 24–34.

ERDAS Inc. 1999. ERDAS IMAGINE field guide. ERDAS Inc., Atlanta, Ga.

Fang, J.Y., and Wang, Z.M. 2001. Forest biomass estimation at regional and global levels, with special reference to China's forest biomass. Ecol. Res. **16**: 587–592.

Fang, J.Y., Chen, A.P., Peng, C.H., Zhao, S.Q., and Ci, L. 2001. Changes in forest biomass carbon storage in China between 1949 and 1998. Science (Washington, D.C.), **292**: 2320–2322.

Fensham, R.J., Fairfax, R.J., Holman, J.E., and Whitehead, P.J. 2002. Quantitative assessment of vegetation structural attributes from aerial photography. Int. J. Remote Sens. **23**: 2293–2317.

Gong, P., Sheng, Y., and Biging, G.S. 2002. 3D model-based tree measurement from high-resolution aerial imagery. Photogramm. Eng. Remote Sens. **68**: 1203–1212.

Grünzweig, J.M., Lin, T., Rotenberg, E., Schwartz, A., and Yakir, D. 2003. Carbon sequestration in arid-land forest. Global Change Biol. **9**: 791–799.

Hudak, A.T., and Wessman, C.A. 1998. Textural analysis of historical aerial photography to characterize woody plant encroachment in South Africa. Remote Sens. Environ. **66**: 317–330.

Hutley, L.B., Leuning, R., Beringer, J., and Cleugh, H.A. 2005. The utility of the eddy covariance techniques as a tool in carbon accounting: tropical savanna as a case study. Aust. J. Bot. **53**: 663–675.

Janssens, I.A., Freibauer, A., Ciais, P., Smith, P., Nabuurs, G.J., Folberth, G., Schlamadinger, B., Hutjes, R.W.A., Ceulemans, R., Schulze, E.D., Valentini, R., and Dolman, A.J. 2003. Europe's terrestrial biosphere absorbs 7 to 12% of European anthropogenic CO_2 emissions. Science (Washington, D.C.), **300**: 1538–1542.

Kadmon, R., and Harari-Kremer, R. 1999. Studying long-term vegetation dynamics using digital processing of historical aerial photographs. Remote Sens. Environ. **68**: 164–176.

Korpela, I.S. 2004. Individual tree measurements by the means of digital aerial photogrammetry. Silva Fenn. Monogr. 3.

Kovats, M. 1997. A large-scale aerial photographic technique for measuring tree heights on long-term forest installations. Photogramm. Eng. Remote Sens. **63**: 741–747.

Larsen, M., and Rudemo, M. 1998. Optimizing templates for finding trees in aerial photography. Pattern Recogn. Lett. **19**: 1153–1162.

Nakashizuka, T., Katsuki, T., and Tanaka, H. 1995. Forest canopy structure analyzed by using aerial photographs. Ecol. Res. **10**: 13–18.

Nelson, R., Krabill, W., and Tonelli, J. 1988. Estimating forest biomass and volume using airborne laser data. Remote Sens. Environ. **24**: 247–267.

Nelson, R., Oderwald, R., and Gregoire, T.G. 1997. Separating the ground and airborne laser sampling phases to estimate tropical forest basal area, volume, and biomass. Remote Sens. Environ. **60**: 311–326.

Okuda, T., Suzuki, M., Numata, S., Yoshida, K., Nishimura, S., Adachi, N., Niiyama, K., Manokaran, N., and Hashim, M. 2004. Estimation of aboveground biomass in logged and primary lowland rainforests using 3-D photogrammetric analysis. For. Ecol. Manage. **203**: 63–75.

Parresol, B.R. 1999. Assessing tree and stand biomass: a review with examples and critical comparisons. For. Sci. **45**: 573–593.

Ranson, K.J., Sun, G., Weishampel, J.F., and Knox, R.G. 1997. Forest biomass from combined ecosystem and radar backscatter modeling. Remote Sens. Environ. **59**: 118–133.

Ritson, P., and Sochacki, S. 2003. Measurement and prediction of biomass and carbon content of *Pinus pinaster* trees in a farm forestry plantations, south-western Australia. For. Ecol. Manage. **175**: 103–117.

Seeber, G. 1993. Satellite geodesy: foundations, methods and applications. Walter de Gruyter, New York.

Son, Y., Hwang, J.W., Kim, Z.S., Lee, W.K., and Kim, J.S. 2001. Allometry and biomass of Korean pine (*Pinus koreainesis*) in central Korea. Bioresour. Technol. **78**: 251–255.

Sprugel, D.G. 1983. Correcting for bias in log-transformed allometric equations. Ecology, **64**: 209–210.

St-Onge, B., Jumelet, J., Cobello, M., and Vega, C. 2004. Measuring individual tree height using a combination of stereophotogrammetry and lidar. Can. J. For. Res. **34**: 2122–2130.

Svoray, T., and Shoshany, M. 2003. Herbaceous biomass retrieval in habitats of complex composition: a model merging SAR images with unmixed Landsat data. IEEE Trans. Geosci. Remote Sens. **41**: 1592–1601.

Treuhaft, R.N., Asner, G.P., and Law, B.E. 2003. Structure-based forest biomass from fusion of radar and hyperspectral observations. Geophys. Res. Lett. **30**: 1472. doi: 10.1029/2002GL016857.

Tsolomon, R., Tateishi, R., and Tetuko, J. 2002. A method to estimate forest biomass and its application to monitor Mongolian taiga using JERS-1 SAR data. Int. J. Remote Sens. **23**: 4971–4978.

Valentini, R., Matteucci, G., Dolman, A.J., Schulze, E.D., Rebmann, C., Moors, E.J., Granier, A., Gross, P., Jensen, N.O., Pilegaard, K., Ceulemans, R., Kowalski, A.S., Vesala, T., Rannik, U., Berbigier, P., Loustau, D., Guomundsson, J.,

Thorgeirsson, H., Ibrom, A., Morgenstern, K., Clement, R., Moncrieff, J., Montagnani, L., Minerbi, S., and Jarvis, P.G. 2000. Respiration as the main determinant of carbon balance in European forests. Nature (London), **404**: 861–865.

Waring, R.H., and Schlesinger, W.H. 1985. Forest ecosystems. Academic Press, London, UK.

West, G.B., Brown, J.H., and Enquist, B.J. 1997. A general model for the origin of allometric scaling laws in biology. Science (Washington, D.C.), **276**: 122–126.